INTERNATIONAL JOURNAL FOR NUMERICAL METHODS IN FLUIDS, VOL. 13, 1267–1287 (1991)

A FINITE ELEMENT FORMULATION FOR LAMINAR FLOW OF A FLUID WITH MICROSTRUCTURE

H. A. HOGAN

Department of Mechanical Engineering, Texas A&M University, College Station, TX 77843, U.S.A.

AND

M. HENRIKSEN

Department of Engineering, Colorado School of Mines, Golden, CO 80401, U.S.A.

SUMMARY

A finite element formulation for the steady laminar flow of an incompressible fluid with microstructure has been developed. The particular fluids considered are commonly known as micropolar fluids, in which case suspended particulate microstructures are modelled by an 'extended' continuum formulation. The particle microspin is a new kinematic variable which is independent of the classical vorticity vector and thereby allows relative rotation between particles and the surrounding fluid. This formulation also gives rise to couple stresses in addition to classical force or traction stresses. The finite element formulation utilizes a variational approach and imposes conservation of mass through a penalty function. A general boundary condition for microspin has been incorporated whereby microspin at a solid boundary is constrained to be proportional to the fluid vorticity. The proportionality constant in this case can vary from zero to unity. Sample solutions are presented for fully developed flow through a straight tube and compared with an analytical solution. Results are also generated for flow through a constricted tube and compared with a Newtonian fluid solution.

KEY WORDS Micropolar fluid Finite element formulation Laminar flow Constricted tube

INTRODUCTION

One of the basic assumptions of classical continuum theory is that materials remain homogeneous as the size of any arbitrary volume element decreases to a point. Real materials, however, are composed of discrete, finite components at the microstructural level and therefore sometimes exhibit behaviour that classical theory is unable to describe adequately. Consequently, various attempts have been made to 'extend' or 'generalize' classical continuum theory with the intent of capturing a broader range of response phenomena. Although pioneering work was done much earlier,[1–3] renewed interest in this topic began rather intensely in the early 1960s.[4–8] While these efforts to 'extend' or 'generalize' classical theory differ in many respects, they share a common purpose in seeking to expand the range of applicability of the theory while retaining a *continuum* approach because of its inherent elegance and mathematical tractability.

An approach frequently taken in extending classical continuum theory has been to introduce higher-order kinematic variables. The simplest form of this approach is to consider each particle of a material to have a rotation that is independent of the classical rotation. This allows each microstructural 'particle' to have a relative rotation with respect to the surrounding material. The

0271–2091/91/201267–21$10.50

Received 19 April 1990
Revised 22 February 1991

same basic theory has been developed by several workers using different conceptual frameworks and notations. One of the more widely cited and researched is the so-called 'micropolar' theory of Eringen.[9,10] Details of the original developments of micropolar and similar theories are well documented in the literature.[11-14] Recently, an entire textbook has been devoted to the subject of higher-order theories for non-classical fluids;[15] in this treatment an excellent overview of micropolar fluids is presented as a subclass of more complex theories.

Physical problems that have attracted attention as possible applications of micropolar fluids typically involve the flow of fluids containing suspended particles. Human blood contains red blood cells and has therefore been studied extensively as a micropolar fluid.[16-23] Squeeze film lubrication has also been treated as flow of a micropolar fluid.[24-26] Micropolar fluids and similar higher-order theories have even been applied to modelling turbulence, in which case the microstructure is considered to be fluid eddies.[27,28]

Despite the substantial level of effort that has been focused on micropolar fluids, very few studies have examined problems for which analytical solutions could not be derived. Sastry and Rao[29] developed a specialized numerical technique for the laminar flow of a micropolar fluid in the entrance region of a porous channel. Solutions were generated by combining quasi-linearization, parametric differentiation and extrapolation procedures. Akay and Kaye[30] used finite differences to study the non-steady flow of a two-phase model for blood. Their model consisted of a micropolar fluid core surrounded by a concentric outer layer of a Newtonian fluid. The many advantages of finite element analysis, however, have yet to be exploited in studying the flow of micropolar fluids. The discussion to follow describes a finite element formulation that permits the investigation of much more general and complex problems involving the flow of micropolar fluids.

MICROPOLAR FLUID THEORY

The distinguishing feature of micropolar theory is the introduction of a particle rotation that is independent of the classical rotation. This kinematic variable is referred to as the microrotation. For a physical interpretation one may treat the micropolar fluid as a fluid containing suspended particles. The microrotation is then considered to be the rotation of the particles, while the classical rotation describes the rotation of the surrounding fluid. The existence of particle microrotation also gives rise to couple stresses or couples per unit area, in addition to traditional tractional or force stresses. Excellent detailed descriptions and discussions of micropolar fluids are presented in References 9 and 14.

The three balance laws of micropolar fluid mechanics are conservation of mass, conservation of linear momentum and conservation of angular momentum. The first two are similar in form to those for classical fluid mechanics. The notation used here follows closely that of Eringen.[9] Letting ρ denote mass density, τ time, x_i Cartesian spatial co-ordinates and v_i components of the velocity vector, the localized form of conservation of mass is given by

$$\frac{\partial \rho}{\partial \tau} + \frac{\partial}{\partial x_i}(\rho v_i) = 0. \tag{1}$$

With components of the body force vector given by f_i and components of the tractional stress tensor by σ_{ji}, conservation of linear momentum becomes

$$\sigma_{ji,j} + \rho(f_i - \dot{v}_i) = 0. \tag{2}$$

The overdot notation on the acceleration term $\dot{v}_i$ indicates a material derivative which includes

both 'local' and 'convective' terms, as evident in the expanded form

$$\dot{v}_i = \frac{\partial v_i}{\partial \tau} + v_{i,j} v_j. \tag{3}$$

The new kinematic quantity, the microrotation, which is characteristic of micropolar fluids, enters into the conservation of angular momentum expression. The rate of microrotation is termed the microspin and is denoted v_j, and $\dot{v}_j$ represents the rate of microspin or angular acceleration. Two other new quantities, the couple stress tensor (m_{ji}) and the microinertia tensor (J_{ji}), also appear in the expression for conservation of angular momentum, which is given in equation form by

$$m_{ji,j} + e_{ikn}\sigma_{kn} + \rho(l_i - J_{ji}\dot{v}_j) = 0. \tag{4}$$

Note that body couples, i.e. couples per unit mass, are denoted by l_i, and e_{ikn} represents the permutation tensor. The microinertia (J_{ji}) of a particle is a second-order tensor and is loosely analogous to the moment of inertia of a rigid body. Thus a physical interpretation of the last term in equation (4) is that it represents the angular momentum of each of the suspended particles. Recall that only the second term appears for classical fluids in the absence of body couples, in which case conservation of angular momentum simply imposes symmetry of the force stress tensor. The overdot again denotes a material derivative as follows:

$$\dot{v}_j = \frac{\partial v_j}{\partial \tau} + v_{j,i} v_i. \tag{5}$$

Appropriate constitutive relations for a linear, isotropic and incompressible micropolar fluid are given by equations (6) and (7) below, where p is the fluid pressure and δ_{ij} is the familiar Kronecker delta. In addition to the shear viscosity μ, four new viscosity coefficients, κ, α, β and γ, are introduced:

$$\sigma_{ij} = -p\delta_{ij} + (\mu + \kappa)\dot{\varepsilon}_{ij} + \mu\dot{\varepsilon}_{ij}, \tag{6}$$

$$m_{ij} = \alpha v_{k,k}\delta_{ij} + \beta v_{i,j} + \gamma v_{j,i}. \tag{7}$$

The rate of microstrain, $\dot{\varepsilon}_{ij}$, is also a quantity unique to extended continuum mechanics. In its most direct form the rate of microstrain is given by equation (8) in terms of microspin and velocity gradients. An alternative expression is presented in equation (9), which relates the microstrain rate to the traditional strain rate $\dot{E}_{ij}$, the traditional vorticity ω_k and the microspin v_k:

$$\dot{\varepsilon}_{ij} = e_{ijk} v_k + v_{j,i}, \tag{8}$$

$$\dot{\varepsilon}_{ij} = \dot{E}_{ij} + e_{ijk}(\omega_k - v_k). \tag{9}$$

Substituting equation (9) into equation (6) yields a similar alternative form for the tractional stress constitutive relation:

$$\sigma_{ij} = -p\delta_{ij} + (2\mu + \kappa)\dot{E}_{ij} + \kappa e_{ijk}(\omega_k - v_k). \tag{10}$$

Note that the last term contains the expression $\omega_k - v_k$, which represents the rate of rotation of the fluid, ω_k, relative to the rate of rotation of the microconstituent particle, v_k. As in the classical case, ω_k is the fluid vorticity vector and is given by

$$\omega_k = \tfrac{1}{2} e_{nmk} v_{m,n}. \tag{11}$$

It is also apparent that the last term in equation (10) accounts for coupling between microspin and force stress. The second term in this equation indicates that the micropolar counterpart for

the traditional shear viscosity is $\mu+\kappa/2$. In the absence of micropolar effects, i.e. when $\kappa=0$, equation (10) degenerates to the constitutive model for classical Newtonian fluids. This form of the expression for σ_{ij} also serves to highlight that the force stress tensor is no longer symmetric for micropolar fluids.

Field equations are generated by substituting the constitutive equations for force stress, equation (6), and couple stress, equation (7), into the expressions for conservation of linear momentum and angular momentum, equations (2) and (4), respectively. Thus the two field equations describing the behaviour of a linear, isotropic, incompressible micropolar fluid are

$$-p_{,i}+\mu v_{j,ji}+(\mu+\kappa)v_{i,jj}+\kappa e_{ijk}v_{k,j}+\rho(f_i-\dot{v}_i)=0, \tag{12}$$

$$(\alpha+\beta)v_{j,ji}+\gamma v_{i,jj}+\kappa e_{ijk}v_{k,j}-2\kappa v_i+\rho(l_i-J\dot{v}_i)=0. \tag{13}$$

Equation (12) reduces to the traditional Navier–Stokes equation for $\kappa=0$. Note as well that equation (13) includes the simplification that the microinertia tensor is isotropic, i.e.

$$J_{ji}=J\delta_{ji}. \tag{14}$$

Boundary conditions are needed for both velocities and microspin in order to solve equations (12) and (13) for a specific problem. For velocities the conventional no-slip condition is employed at solid boundaries, in which case the fluid velocity is taken to be equal to the velocity of the boundary. A proper boundary condition for microspin is not readily apparent. The approach adopted here follows closely that of Kline *et al.*,[22] Erdogan[12] and more recently Chaturani and co-workers.[16,17] The microspin at a solid boundary, v_i^b, is related to the fluid vorticity vector, ω_i^b, by an adjustable parameter S as indicated by

$$v_i^b=S\omega_i^b. \tag{15}$$

No compelling theoretical argument or experimental evidence suggesting a correct value for S has been found in the literature. Its use simply provides a flexible approach, with the unfortunate side effect of essentially introducing another variable into the problem.

FINITE ELEMENT FORMULATION

Variational approach

A variational statement of the problem can be developed by multiplying the conservation of linear and angular momentum equations by suitable trial functions and integrating over the spatial domain of interest (V). The trial functions must be continuous and satisfy essential boundary conditions. For the linear momentum equation the trial function is taken to be the variation of velocity, δv_i, so equation (2) becomes

$$\int_V [\sigma_{ji,j}+\rho(f_i-\dot{v}_i)]\delta v_i \,\mathrm{d}V=0. \tag{16}$$

For steady state analysis, $\dot{v}_i$ reduces to the convection terms only, i.e. the product of velocity gradients $v_{i,j}$ and velocities v_j, as apparent from equation (3). The non-linearity introduced by these terms can be handled using a variety of approaches, such as Newton–Raphson or modified Newton methods, but a direct iteration scheme has been employed here for simplicity. In this case the velocity components v_j are considered to be known and denoted v_j^0, and the gradient terms $v_{i,j}$ remain unknown. The problem can then be solved and the new velocities used for v_j^0. The procedure is then repeated, updating v_j^0 until sufficient convergence is attained.

Treating the acceleration terms in equation (16) as linear since v_j° is assumed known, the Gauss theorem can be applied in the usual manner. With appropriate simplification the following weak form expression results:

$$\int_V \sigma_{ji}\delta v_{i,j}\,\mathrm{d}V=\int_S t_i\delta v_i\,\mathrm{d}S+\int_V \rho f_i\delta v_i\,\mathrm{d}V-\int_V \rho v_{i,j}v_j^\circ\delta v_i\,\mathrm{d}V. \tag{17}$$

Note that the force traction vector $t_i=\sigma_{ji}n_j$ has been introduced, where n_j represents direction cosines of the unit outer normal to surface S.

For angular momentum the trial function is the variation of microspin, δv_i, and equation (4) becomes

$$\int_V [m_{ji,j}+e_{ikn}\sigma_{kn}+\rho(l_i-J_{ji}\dot{v}_j)]\delta v_i\,\mathrm{d}V=0. \tag{18}$$

Assuming steady state conditions and isotropy of microinertia (i.e. $J_{ji}=J\delta_{ji}$), the acceleration term reduces to the product of $v_{i,j}$ and v_j. Taking the velocity components to be known (v_j°) for each solution, applying the Gauss theorem and manipulating yields

$$\int_V m_{ji}\delta v_{i,j}\,\mathrm{d}V-\int_V e_{ikn}\sigma_{kn}\delta v_i\,\mathrm{d}V=\int_S b_i\delta v_i\,\mathrm{d}S+\int_V \rho l_i\delta v_i\,\mathrm{d}V-\int_V \rho J v_{i,j}v_j^\circ\delta v_i\,\mathrm{d}V. \tag{19}$$

In this case the couple stress traction vector $b_i=m_{ji}n_j$, which acts on surface S, is also introduced.

Element equations

To begin development of element equations, the domain is discretized into finite elements. The two primary unknowns, velocities and microspin, are then interpolated over each element. Thus for any particular element the velocity and microspin vector components are given by

$$v_i^e=\sum_{m=1}^{n} h_m\hat{v}_i^m, \qquad v_i^e=\sum_{m=1}^{n} h_m\hat{v}_i^m, \tag{20}$$

where h_m are interpolation functions defined in local co-ordinates over the domain of each element, $\hat{v}_i^m$ and $\hat{v}_i^m$ are respective values for velocity and microspin components at each node, and n is typically the number of nodes in an element.

A frequently employed method to treat the pressure term in the constitutive equation for force stress, and to impose conservation of mass at the same time, is to introduce a penalty parameter λ as developed by Reddy.[31] Taking this approach, and also substituting the rate of microstrain from equation (8) into equation (6), the force stress constitutive equation takes the form

$$\sigma_{ij}=\lambda v_{k,k}\delta_{ij}+(\mu+\kappa)(e_{ijk}v_k+v_{j,i}). \tag{21}$$

Substituting the expressions from equation (20), the force stress over an element is given by

$$\sigma_{ij}^e=\lambda\left(\sum_{m=1}^{n} h_{m,k}\hat{v}_k^m\right)\delta_{ij}+(\mu+\kappa)\left[e_{ijk}\left(\sum_{m=1}^{n} h_m\hat{v}_k^m\right)+\left(\sum_{m=1}^{n} h_{m,i}\hat{v}_j^m\right)\right]. \tag{22}$$

Writing the stress components in a single column vector $\boldsymbol{\sigma}^e$, this equation can be expressed in matrix form as

$$\boldsymbol{\sigma}^e=(\lambda\mathbf{C}_1+\mathbf{C}_2)\mathbf{B}\hat{\mathbf{v}}+\mathbf{C}_3\mathbf{H}_v\hat{\mathbf{v}} \tag{23}$$

where $\mathbf{C}_1$ contains ones and zeros, $\mathbf{C}_2$ and $\mathbf{C}_3$ contain material constants (μ and κ), $\mathbf{B}$ contains

derivatives of interpolation functions, and $\mathbf{H}_v$ contains interpolations functions. With a view towards expressing the variational statement of equation (17) in matrix form, the velocity variation and gradient of velocity variation vectors can be written in matrix form as

$$\delta \mathbf{v} = \mathbf{H}\delta\hat{\mathbf{v}}, \qquad \delta \mathbf{v}_g = \mathbf{B}\delta\hat{\mathbf{v}}, \tag{24}$$

where $\delta\mathbf{v}$ is a vector containing the components of the variation of velocity, δv_i, $\delta\hat{\mathbf{v}}$ is a vector containing nodal values of these same quantities, $\delta\mathbf{v}_g$ is a vector containing components of the velocity gradient variation, $\delta v_{i,j}$, and $\mathbf{H}$ is a matrix containing interpolation functions.

The variational statement associated with linear momentum, equation (17), can now be written in matrix form as

$$\int_V \delta\hat{\mathbf{v}}^T\mathbf{B}^T\boldsymbol{\sigma}^e \,dV = \int_S \delta\hat{\mathbf{v}}^T\mathbf{H}^T\mathbf{t}\,dS + \int_V \rho\delta\hat{\mathbf{v}}^T\mathbf{H}^T\mathbf{f}\,dV - \int_V \rho\delta\hat{\mathbf{v}}^T\mathbf{H}^T\mathbf{B}_c\hat{\mathbf{v}}\,dV, \tag{25}$$

where $\mathbf{B}_c$ is a matrix containing a combination of derivatives of interpolation functions and known velocities from a previous solution. Substituting the expression for force stress from equation (23) into equation (25), rearranging terms and factoring out $\delta\hat{\mathbf{v}}^T$ yields

$$\delta\hat{\mathbf{v}}^T\left(\int_V \lambda\mathbf{B}^T\mathbf{C}_1\mathbf{B}\hat{\mathbf{v}}\,dV + \int_V \mathbf{B}^T\mathbf{C}_2\mathbf{B}\hat{\mathbf{v}}\,dV + \int_V \mathbf{B}^T\mathbf{C}_3\mathbf{H}_v\hat{\mathbf{v}}\,dV + \int_V \rho\mathbf{H}^T\mathbf{B}_c\hat{\mathbf{v}}\,dV - \int_S \mathbf{H}^T\mathbf{t}\,dS - \int_V \rho\mathbf{H}^T\mathbf{f}\,dV\right) = 0. \tag{26}$$

Since the variation of velocity is arbitrary, the term in parentheses must vanish for equation (26) to hold. Nodal velocities and microspins are constant with respect to integration over the domain of each element, so the resulting expression can be written as

$$(\mathbf{K}_1 + \mathbf{K}_2 + \mathbf{K}_c)\hat{\mathbf{v}} + \mathbf{K}_3\hat{\mathbf{v}} = \mathbf{r}_1 + \mathbf{r}_2, \tag{27}$$

where

$$\mathbf{K}_1 = \int_V \lambda\mathbf{B}^T\mathbf{C}_1\mathbf{B}\,dV, \tag{27a}$$

$$\mathbf{K}_2 = \int_V \mathbf{B}^T\mathbf{C}_2\mathbf{B}\,dV, \tag{27b}$$

$$\mathbf{K}_c = \int_V \rho\mathbf{H}^T\mathbf{B}_c\,dV, \tag{27c}$$

$$\mathbf{K}_3 = \int_V \mathbf{B}^T\mathbf{C}_3\mathbf{H}_v\,dV, \tag{27d}$$

$$\mathbf{r}_1 = \int_S \mathbf{H}^T\mathbf{t}\,dS, \tag{27e}$$

$$\mathbf{r}_2 = \int_V \rho\mathbf{H}^T\mathbf{f}\,dV. \tag{27f}$$

Equation (27) can be further simplified by forming a single, partitioned coefficient matrix

$$\underset{(2n\times 2n)}{[(\mathbf{K}_1+\mathbf{K}_2+\mathbf{K}_c)}\,|\,\underset{(2n\times n)}{(\mathbf{K}_3)}\,]\underset{(3n\times 1)}{\left\{\begin{matrix}\hat{\mathbf{v}}\\ \hline \dot{\hat{\mathbf{v}}}\end{matrix}\right\}} = \underset{(2n\times 1)}{\{\mathbf{r}_1+\mathbf{r}_2\}} \tag{28}$$

or

$$\underset{(2n\times 3n)}{[\mathbf{K}_v^e]} \underset{(3n\times 1)}{\left\{\begin{matrix}\hat{\mathbf{v}}\\ \hat{v}\end{matrix}\right\}} = \underset{(2n\times 1)}{\{\mathbf{r}_v^e\}}. \tag{29}$$

The dimensions of the matrices and vectors have been added for clarity for the case of n nodes per element, two velocity components and one microspin component (two-dimensional flow).

This entire procedure is repeated for the angular momentum equation, beginning with an expression for couple stress over an element. Referring again to equation (20) for velocity and microspin over an element, the couple stress from equation (7) can be expressed as

$$m_{ij}^e = \alpha\left(\sum_{m=1}^{n} h_{m,k}\,\hat{v}_k^m\right)\delta_{ij} + \beta\left(\sum_{m=1}^{n} h_{m,j}\,\hat{v}_i^m\right) + \gamma\left(\sum_{m=1}^{n} h_{m,i}\,\hat{v}_j^m\right). \tag{30}$$

In matrix form the components of couple stress are arranged in a single column vector, which is given by

$$\mathbf{m}^e = \mathbf{C}_4\mathbf{B}_v\hat{v}, \tag{31}$$

where $\mathbf{C}_4$ is a matrix containing constitutive constants (α, β and γ) and $\mathbf{B}_v$ contains spatial derivatives of interpolation functions. Variations of microspin and microspin gradients can also be expressed in matrix form as

$$\delta v = \mathbf{H}_v\delta\hat{v}, \qquad \delta v_g = \mathbf{B}_v\delta\hat{v}, \tag{32}$$

where δv is a vector containing the components of the variation of microspin, δv_i, $\delta\hat{v}$ is a vector containing nodal values of these same quantities and δv_g, is a vector containing components of the variation of microspin gradient, $\delta v_{i,j}$. The matrices $\mathbf{H}_v$ and $\mathbf{B}_v$ contain interpolation functions and their derivatives, respectively.

The variational statement associated with angular momentum, equation (19), can also be written in matrix form. First, the effect of the permutation tensor e_{ikn} in the second term is represented by a square matrix $\mathbf{P}$ which contains ones and zeros and includes the negative sign preceding this term. Equation (19) then becomes

$$\int_V \delta\hat{v}^{\mathrm{T}}\mathbf{B}_v^{\mathrm{T}}\mathbf{m}^e\,\mathrm{d}V + \int_V \delta\hat{v}^{\mathrm{T}}\mathbf{H}_v^{\mathrm{T}}\mathbf{P}\sigma^e\,\mathrm{d}V = \int_S \delta\hat{v}^{\mathrm{T}}\mathbf{H}_v^{\mathrm{T}}\mathbf{b}\,\mathrm{d}S + \int_V \rho\delta\hat{v}^{\mathrm{T}}\mathbf{H}_v^{\mathrm{T}}\mathbf{l}\,\mathrm{d}V - \int_V \rho J\delta\hat{v}^{\mathrm{T}}\mathbf{H}_v^{\mathrm{T}}\mathbf{B}_c'\hat{v}\,\mathrm{d}V. \tag{33}$$

Note that the simplified convective acceleration terms are included through the matrix $\mathbf{B}_c'$ which appears in the last term. As before, this matrix contains a combination of interpolation function derivatives and velocity components from a previous iteration. Substituting the constitutive relations for force stress, equation (23), and couple stress, equation (31), into the left-hand side of equation (33), rearranging terms and factoring out $\delta\hat{v}^{\mathrm{T}}$ yields

$$\delta\hat{v}^{\mathrm{T}}\left(\int_V \mathbf{B}_v^{\mathrm{T}}\mathbf{C}_4\mathbf{B}_v\hat{v}\,\mathrm{d}V + \int_V \lambda\mathbf{H}_v^{\mathrm{T}}\mathbf{P}\mathbf{C}_1\mathbf{B}\hat{v}\,\mathrm{d}V + \int_V \mathbf{H}_v^{\mathrm{T}}\mathbf{P}\mathbf{C}_2\mathbf{B}\hat{v}\,\mathrm{d}V + \int_V \mathbf{H}_v^{\mathrm{T}}\mathbf{P}\mathbf{C}_3\mathbf{H}_v\hat{v}\,\mathrm{d}V + \int_V \rho J\mathbf{H}_v^{\mathrm{T}}\mathbf{B}_c'\hat{v}\,\mathrm{d}V - \int_S \mathbf{H}_v^{\mathrm{T}}\mathbf{b}\,\mathrm{d}S - \int_V \rho\mathbf{H}_v^{\mathrm{T}}\mathbf{l}\,\mathrm{d}V\right) = 0. \tag{34}$$

The variation of microspin is also arbitrary, so the term in parentheses is again forced to vanish. With nodal velocities and microspins factored out of the integrals, equation (34) can be rewritten as

$$(\mathbf{K}_4+\mathbf{K}_5)\hat{v} + (\mathbf{K}_6+\mathbf{K}_7+\mathbf{K}_c')\hat{v} = \mathbf{r}_3+\mathbf{r}_4, \tag{35}$$

where

$$\mathbf{K}_4 = \int_V \lambda \mathbf{H}_v^T \mathbf{P} \mathbf{C}_1 \mathbf{B} \, dV, \tag{35a}$$

$$\mathbf{K}_5 = \int_V \mathbf{H}_v^T \mathbf{P} \mathbf{C}_2 \mathbf{B} \, dV, \tag{35b}$$

$$\mathbf{K}_6 = \int_V \mathbf{B}_v^T \mathbf{C}_4 \mathbf{B}_v \, dV, \tag{35c}$$

$$\mathbf{K}_7 = \int_V \mathbf{H}_v^T \mathbf{P} \mathbf{C}_3 \mathbf{H}_v \, dV, \tag{35d}$$

$$\mathbf{K}_c' = \int_V \rho J \mathbf{H}_v^T \mathbf{B}_c' \, dV, \tag{35e}$$

$$\mathbf{r}_3 = \int_S \mathbf{H}_v^T \mathbf{b} \, dS, \tag{35f}$$

$$\mathbf{r}_4 = \int_V \rho \mathbf{H}_v \mathbf{l} \, dV, \tag{35g}$$

Simplifying equation (35) and including matrix dimensions again produces the following form:

$$\underset{(n\times 2n)}{[(\mathbf{K}_4+\mathbf{K}_5)\,|\,(\mathbf{K}_6+\mathbf{K}_7+\mathbf{K}_c')]} \underset{(3n\times 1)}{\left\{\begin{matrix}\hat{\mathbf{v}}\\ \hline \hat{\mathbf{v}}\end{matrix}\right\}} = \underset{(n\times 1)}{\{\mathbf{r}_3+\mathbf{r}_4\}} \tag{36}$$

or

$$\underset{(n\times 3n)}{[\mathbf{K}_v^e]} \underset{(3n\times 1)}{\left\{\begin{matrix}\hat{\mathbf{v}}\\ \hline \hat{\mathbf{v}}\end{matrix}\right\}} = \underset{(n\times 1)}{\{\mathbf{r}_v^e\}}. \tag{37}$$

A single element equation can now be formed by combining equations (29) and (37) to give

$$\underset{(3n\times 3n)}{\left[\begin{matrix}\mathbf{K}_v^e\\ \hline \mathbf{K}_v^e\end{matrix}\right]} \underset{(3n\times 1)}{\left\{\begin{matrix}\hat{\mathbf{v}}\\ \hline \hat{\mathbf{v}}\end{matrix}\right\}} = \underset{(3n\times 1)}{\left\{\begin{matrix}\mathbf{r}_v^e\\ \hline \mathbf{r}_v^e\end{matrix}\right\}} \tag{38}$$

or

$$[\mathbf{K}^e]\left\{\begin{matrix}\hat{\mathbf{v}}\\ \hline \hat{\mathbf{v}}\end{matrix}\right\} = \{\mathbf{r}^e\}. \tag{39}$$

Assembly and boundary conditions

Element equations are assembled in the usual manner to form a single matrix equation for the entire domain or system. Element coefficient matrices are combined to form the coefficient matrix for the system, **K**, and the vectors **v** and ***v*** now represent nodal unknowns for the entire system:

$$[\mathbf{K}]\left\{\begin{matrix}\mathbf{v}\\ \hline \boldsymbol{v}\end{matrix}\right\} = \{\mathbf{r}\}. \tag{40}$$

Essential boundary conditions in the form of specified velocities and/or microspins are imposed in a typical manner. Specified velocities ($\mathbf{v}_{bc}$) and/or microspins (v_{bc}) are eliminated from the vector of nodal unknowns, the coefficient matrix is reduced accordingly and, for non-zero essential boundary conditions, the right-hand-side vector is augmented by the product of each known value and the corresponding column of the coefficient matrix. The modified system equation becomes

$$[\mathbf{K}_{vv}]\left\{\begin{matrix}\mathbf{v}_{ue}\\ \hline v_{ue}\end{matrix}\right\}=\{\mathbf{r}\}-[\mathbf{K}_{ebc}]\left\{\begin{matrix}\mathbf{v}_{bc}\\ \hline v_{bc}\end{matrix}\right\}=\{\mathbf{r}_{ebc}\}, \tag{41}$$

where $\mathbf{K}_{vv}$ is the reduced coefficient matrix, $\mathbf{v}_{ue}$ and v_{ue} are vectors containing the remaining unknown velocities and microspins, respectively, and $\mathbf{K}_{ebc}$ is a matrix containing appropriate columns of the original coefficient matrix. Natural boundary conditions are also imposed in a customary manner. The right-hand-side vector $\mathbf{r}$ is formed as an assemblage of contributions from each element vector $\mathbf{r}^e$. This element right-hand-side vector contains contributions from both surface tractions (force stress and couple stress) and body forces ($\mathbf{f}$) and couples ($\mathbf{l}$). Natural boundary conditions are therefore implemented on an element-by-element basis by evaluating the surface integral vectors: $\mathbf{r}_1$ for specified force stress tractions ($\mathbf{t}$) and $\mathbf{r}_3$ for specified couple stress tractions ($\mathbf{b}$). Expressions for $\mathbf{r}_1$ and $\mathbf{r}_3$ were presented previously in equations (27e) and (35f), respectively. Thus equation (41) includes natural boundary conditions through the vector $\mathbf{r}$.

Boundary conditions for microspin at solid boundaries are specified by equation (15), which states that microspin is related to the vorticity vector. Combining this with the definition of vorticity in terms of velocity gradients, equation (11), yields the following expression relating microspin to velocity gradients at solid boundaries:

$$v_i=(S/2)\mathrm{e}_{ijk}v_{k,j}. \tag{42}$$

This boundary condition for microspin simply amounts to constraining microspin components to be related to velocity components in a prescribed manner. This unconventional boundary condition is actually implemented on an element-by-element basis similar to natural boundary conditions. First, the vector of nodal microspins is partitioned into a vector containing microspin components at points on solid boundaries, $\hat{\mathbf{v}}_s$, and a vector containing the remaining unknown nodal microspins, $\hat{\mathbf{v}}_u$. The cofficient matrix can also be partitioned such that element equation (39) becomes

$$\left[\begin{array}{c|c}\mathbf{K}_{vu} & \mathbf{K}_{vs}\\ \hline \mathbf{K}'_{vu} & \mathbf{K}'_{vs}\end{array}\right]^e\left\{\begin{matrix}\hat{\mathbf{v}}\\ \hline \hat{\mathbf{v}}_u\\ \hline \hat{\mathbf{v}}_s\end{matrix}\right\}=\{\mathbf{r}^e\}, \tag{43}$$

which can be written as two separate matrix equations

$$[\mathbf{K}^e_{vu}]\left\{\begin{matrix}\hat{\mathbf{v}}\\ \hline \hat{\mathbf{v}}_u\end{matrix}\right\}+[\mathbf{K}^e_{vs}]\{\hat{\mathbf{v}}_s\}=\{\mathbf{r}^e_s\}, \tag{44a}$$

$$[\mathbf{K}'^e_{vu}]\left\{\begin{matrix}\hat{\mathbf{v}}\\ \hline \hat{\mathbf{v}}_u\end{matrix}\right\}+[\mathbf{K}'^e_{vs}]\{\hat{\mathbf{v}}_s\}=\{\mathbf{r}'^e_s\}. \tag{44b}$$

If matrix dimensions are included again for the case of 2D flow (i.e. two velocities and one microspin), then the number of 'active' unknowns per element, n_a, is equal to $3n-n_s$, where n_s is the number of nodes on the solid boundary and n is the number of nodes per element. With the

number of 'active' unknown microspins per element denoted n_m (and equal to $n-n_s$), the matrix $\mathbf{K}^e_{vu}$ in equation (44a) can be further partitioned to yield

$$\underset{(n_a\times 2n)}{[\mathbf{K}^e_{vv}]}\ \underset{(2n\times 1)}{\{\hat{\mathbf{v}}\}} + \underset{(n_a\times n_m)}{[\mathbf{K}^e_{vu}]}\ \underset{(n_m\times 1)}{\{\hat{\mathbf{v}}_u\}} + \underset{(n_a\times n_s)}{[\mathbf{K}^e_{vs}]}\ \underset{(n_s\times 1)}{\{\hat{\mathbf{v}}_s\}} = \underset{(n_a\times 1)}{\{\mathbf{r}^e_s\}}\,. \tag{45}$$

The conditions of equation (42) can now be imposed on $\hat{\mathbf{v}}_s$ and expressed in matrix form as

$$\underset{(n_s\times 1)}{\{\hat{\mathbf{v}}_s\}} = S\,\underset{(n_s\times 2n)}{[\mathbf{B}^e_{sbc}]}\ \underset{(2n\times 1)}{\{\hat{\mathbf{v}}\}}\,, \tag{46}$$

where $\mathbf{B}^e_{sbc}$ is a matrix that contains spatial derivatives of interpolation functions and several columns of zeros, since $\hat{\mathbf{v}}$ includes *all* the unknown nodal velocities for the element whereas $\hat{\mathbf{v}}_s$ contains unknown nodal microspins on the solid boundary only. Substituting $\hat{\mathbf{v}}_s$ from equation (46), the third term of equation (45) can be expressed as

$$[\mathbf{K}^e_{vs}]\{\hat{\mathbf{v}}_s\} = [\mathbf{K}^e_{vs}]S[\mathbf{B}^e_{sbc}]\{\hat{\mathbf{v}}\} = [\mathbf{K}^e_{sbc}]\{\hat{\mathbf{v}}\}, \tag{47a}$$

where $\mathbf{K}^e_{sbc}$ is defined by

$$[\mathbf{K}^e_{sbc}] = S[\mathbf{K}^e_{vs}][\mathbf{B}^e_{sbc}]. \tag{47b}$$

Equation (45) can now be rewritten in its entirety as

$$[\mathbf{K}^e_{vv}]\{\hat{\mathbf{v}}\} + [\mathbf{K}^e_{vu}]\{\hat{\mathbf{v}}_u\} + [\mathbf{K}^e_{sbc}]\{\hat{\mathbf{v}}\} = \{\mathbf{r}^e_s\} \tag{48}$$

or, with regrouping of terms,

$$[\mathbf{K}^e_{vv} + \mathbf{K}^e_{sbc}]\{\hat{\mathbf{v}}\} + [\mathbf{K}^e_{vu}]\{\hat{\mathbf{v}}_u\} = \{\mathbf{r}^e_s\}. \tag{49}$$

Defining the matrix $\mathbf{K}^e_{bc}$ by

$$[\mathbf{K}^e_{bc}] = [\mathbf{K}^e_{vv} + \mathbf{K}^e_{sbc}], \tag{50}$$

equation (49) becomes

$$[\mathbf{K}^e_{bc} \mid \mathbf{K}^e_{vu}] \left\{ \begin{array}{c} \hat{\mathbf{v}} \\ \hline \hat{\mathbf{v}}_u \end{array} \right\} = \{\mathbf{r}^e_s\}. \tag{51}$$

Adding matrix dimensions again for clarity and combining the coefficient matrix yields

$$\underset{(n_a\times n_a)}{[\mathbf{K}^e_{vs}]} \underset{(n_a\times 1)}{\left\{ \begin{array}{c} \hat{\mathbf{v}} \\ \hline \hat{\mathbf{v}}_u \end{array} \right\}} = \underset{(n_a\times 1)}{\{\mathbf{r}^e_s\}}\,. \tag{52}$$

In this form the microspins that lie on solid boundaries have been eliminated as independent unknowns and the element coefficient matrix has been reduced in size accordingly. The constraint relating microspin to velocity at the boundaries is included in the appropriate terms of the new coefficient matrix $\mathbf{K}^e_{vs}$.

It should be noted that in the actual computer implementation the derivatives of interpolation functions contained in $\mathbf{B}^e_{sbc}$ are evaluated at the nodes on the solid boundaries. All other terms involving interpolation functions and their derivatives in the element coefficient matrices are calculated in the usual manner at numerical integration points. Furthermore, the original coefficient matrix $\mathbf{K}^e$ need not be explicitly reduced to $\mathbf{K}^e_{vs}$. Essentially the same effect is achieved by simply adding in the constraint terms from $\mathbf{K}^e_{sbc}$ as indicated in equation (50) and then

eliminating microspins on solid boundaries as unknowns in the global, or system level, equations as is done for essential boundary conditions. With this approach employed, equation (41) now becomes

$$[\mathbf{K}'_{vv}]\left\{\frac{\mathbf{v}_{ue}}{\mathbf{v}'_{ue}}\right\}=\{\mathbf{r}_{bc}\}, \tag{53}$$

where $\mathbf{K}'_{vv}$ contains terms reflecting the constraint on microspins at solid boundaries, $\mathbf{v}'_{ue}$ contains all unknown microspins not on solid boundaries or specified through essential boundary conditions, and $\mathbf{r}_{bc}$ has been further reduced by the number of microspins on solid boundaries. In solving this equation, it should be noted that the coefficient matrix $\mathbf{K}'_{vv}$ also contains non-linear terms due to the convective acceleration terms. In addition, the matrix is unsymmetric as a consequence of the asymmetry of the force stress tensor σ_{ij}.

SAMPLE SOLUTIONS

Flow through a straight tube

Problem description. To demonstrate the finite element formulation, example solutions are first presented for the steady flow of a micropolar fluid through a straight tube of circular cross-section. The problem is axisymmetric, so cylindrical co-ordinates are introduced as indicated in the mesh of Figure 1. The angular θ-co-ordinate direction is perpendicular to the r–z plane shown. The mesh of nine-noded Lagrangian elements is refined somewhat as r increases because of higher gradients near the tube wall. Three-by-three Gauss quadrature numerical integration has been used for evaluating most of the coefficient matrices. For the matrix containing the incompressibility constraint the integration order has been reduced to two-by-two.

For axisymmetric, fully developed flow the non-zero primary unknowns reduce to one component of microspin, v_θ, and two components of velocity, v_r and v_z. Appropriate boundary

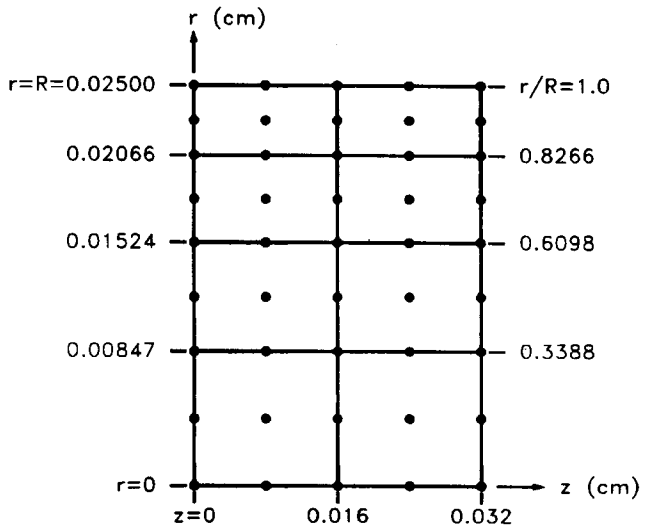

Figure 1. Finite element mesh for sample problem

conditions at the solid boundary ($r=R$) and at the tube centreline ($r=0$) are

$$v_z=v_r=0 \quad \text{at } r=R, \tag{54a}$$

$$v_\theta=S\omega_\theta=(S/2)(v_{r,z}-v_{z,r}) \quad \text{at } r=R, \tag{54b}$$

$$t_z=v_r=v_\theta=0 \quad \text{at } r=0. \tag{54c}$$

The natural boundary condition represented by $t_z=0$ indicates a traction-free condition; for the special case of the tube centreline this amounts to requiring the shear stress component σ_{rz} to vanish. Since v_θ and v_r are also constrained to vanish along this boundary, the condition further reduces to zero velocity gradient or $v_{z,r}=0$. Inlet and outlet boundary conditions are

$$t_z=-P \quad \text{and} \quad b_\theta=v_r=0 \qquad \text{at } z=0, \tag{54d}$$

$$t_z=b_\theta=v_r=0 \qquad \text{at } z=0{\cdot}032 \text{ cm}. \tag{54e}$$

The natural boundary conditions at the inlet and outlet in terms of the force stress traction t_z create a net driving pressure P. The inlet and outlet are both considered to be traction-free in terms of the couple stress traction b_θ, which imposes the fully developed flow condition $v_{\theta,z}=0$.

Values for the constitutive constants have been taken from Ariman *et al.*,[32] who derived them from experimental work by Bugliarello and Sevilla.[33] They are intended to represent the physical properties of blood for a red blood cell concentration of 40%. For axisymmetric flow conditions the micropolar or couple stress constant α is not needed because the term containing this parameter drops out of the constitutive relation for couple stress, equation (7). Thus the values used in the sample solutions are

$$\mu=0{\cdot}0120 \text{ cP}, \tag{55a}$$

$$\kappa=0{\cdot}0196 \text{ cP}, \tag{55b}$$

$$\beta=-12{\cdot}0\times10^{-8} \text{ g cm s}^{-1}, \tag{55c}$$

$$\gamma=12{\cdot}0\times10^{-8} \text{ g cm s}^{-1}, \tag{55d}$$

$$J=0{\cdot}5504\times10^{-5} \text{ cm}. \tag{55e}$$

Recall that the equivalent shear viscosity for a corresponding classical Newtonian fluid is given by

$$\mu+\kappa/2=0{\cdot}0218 \text{ cP}. \tag{56}$$

Results and discussion. Chaturani and Mahajan have solved this problem analytically and provide Bessel function expressions for velocities and microspin in Reference 16. Results generated from these expressions are included in Table I along with finite element results using the present formulation. Maximum axial velocities, which occur at the tube centreline, and microspins at the tube wall are given. The flow rate for all cases has been held constant at $8{\cdot}27\times10^{-3} \text{ cm}^3 \text{ s}^{-1}$, which requires different driving pressures for each case. Finite element solutions typically converged in 8–10 iterations. Plots showing profiles of velocity and microspin as a function of radial location are presented in Figures 2 and 3. Note that plots have been presented for the extreme values of S (0·0 and 1·0) and one intermediate value (0·3525) rather than for all five values of S studied. As evident from Table I and the plots, the finite element solutions agree quite well with analytical results for velocity and microspin. Values for microspin are generally less accurate but differ by no more than 6% from the analytical solution. Accuracy decreases as S approaches zero because of the more extreme microspin gradients near the tube

Table I. Velocity and microspin results

S	Inlet P (dyn cm^{-2})	v_z at $r=0$ (cm s^{-1})		v_θ at $r=R$ (rad s^{-1})	
		Ref. 16	F.E.	Ref. 16	F.E.
0·0	391·3	8·765	8·766	0·0	0·0
0·1663	389·3	8·720	8·722	44·3	46·6
0·3525	386·8	8·664	8·663	98·5	102·6
0·8283	379·3	8·495	8·499	264·6	266·5
1·0	376·0	8·422	8·434	336·9	334·0

Note: the axial location for F.E. results is $z=0{\cdot}016$ cm.

Table II. Shear stresses at tube wall ($r=R$)

S	Inlet P (dyn cm^{-2})	σ_{zr} (dyn cm^{-2})		σ_{rz} (dyn cm^{-2})	
		Ref. 16	F.E.	Ref. 16	F.E.
0·0	391·3	6·14	6·50	16·17	17·11
0·1663	389·3	7·26	7·64	15·97	16·80
0·3525	386·8	8·64	9·00	15·74	16·39
0·8283	379·3	12·86	12·95	15·01	15·11
1·0	376·0	14·69	14·56	14·69	14·56

Note: the axial location for F.E. results is $z=0{\cdot}016$ cm.

wall as a result of greater 'relative rotation' $\omega_\theta - v_\theta$. The vorticity vector ω_θ depends on the velocity field whereas microspin v_θ is being constrained to be a smaller and smaller proportion of ω_θ (see equation (54b)).

Results for shear stresses at the tube wall are summarized in Table II. Once again, values derived from the analytical solution of Chaturani and Mahajan[16] have been included for comparison. Shear stress profile plots are presented in Figures 4 and 5. As is characteristic of micropolar continuum theory, the stress tensor is not symmetric, so the shear stress components are not equal. The special case of $S=1$ is an exception because of zero relative rotation, as can be seen from the alternative form of the force stress constitutive relation, equation (10). Shear stresses are typically not as accurate as the primary variables since they are derived from gradients of these variables. In this case the inaccuracies follow the same pattern as those for microspin: they are greater as S approaches zero, they are greater near the wall, and the maximum percentage difference is slightly less than 6%.

Flow through a constricted tube

Problem description. The finite element formulation has also been used to study the flow of a micropolar fluid through a tube containing a constriction. Like the simpler example, the tube is straight and has a circular cross-section. Unlike the simpler case, however, analytical solutions are not available. The problem is again axisymmetric as depicted in Figure 6. The constriction is formed by a smooth cosine function decrease in tube radius.

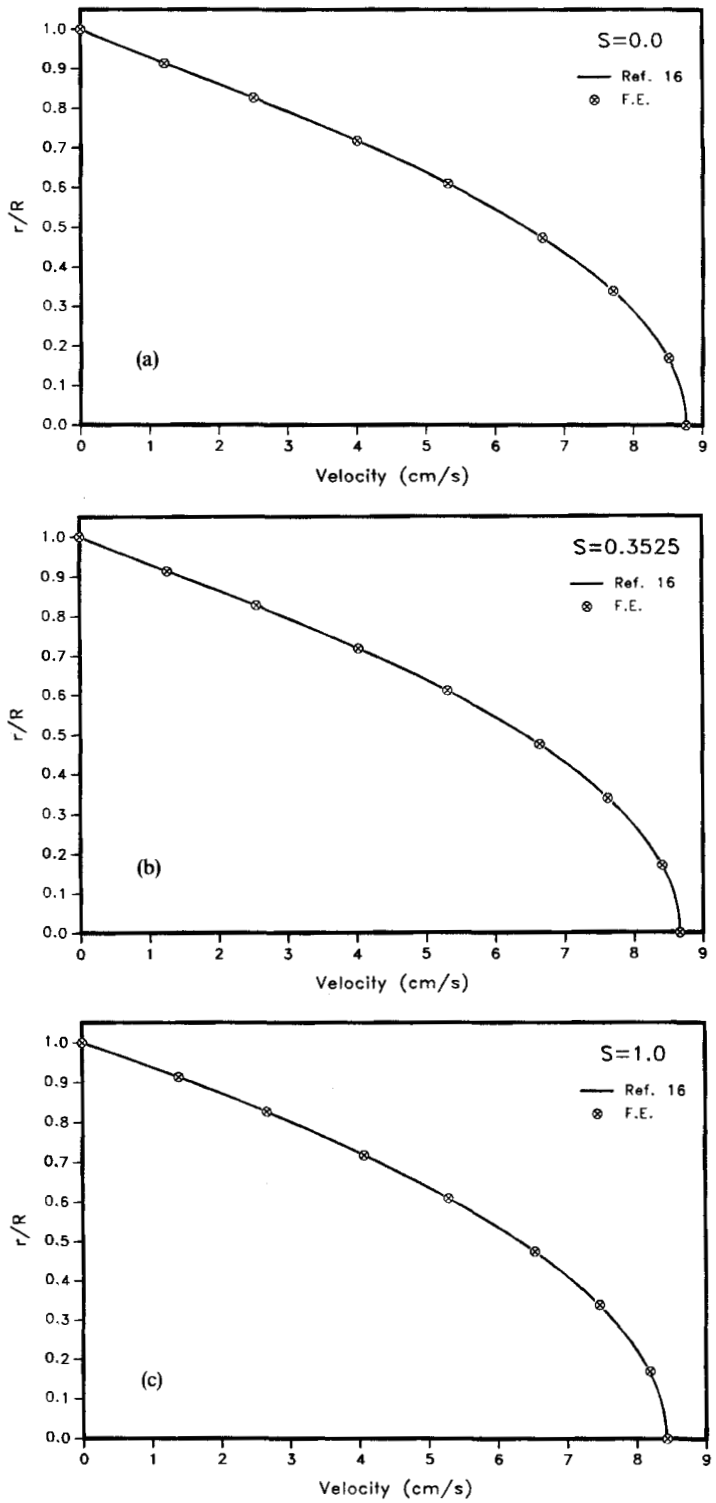

Figure 2. Axial velocity (v_z) profiles for $S=0{\cdot}0$, $0{\cdot}3525$ and $1{\cdot}0$

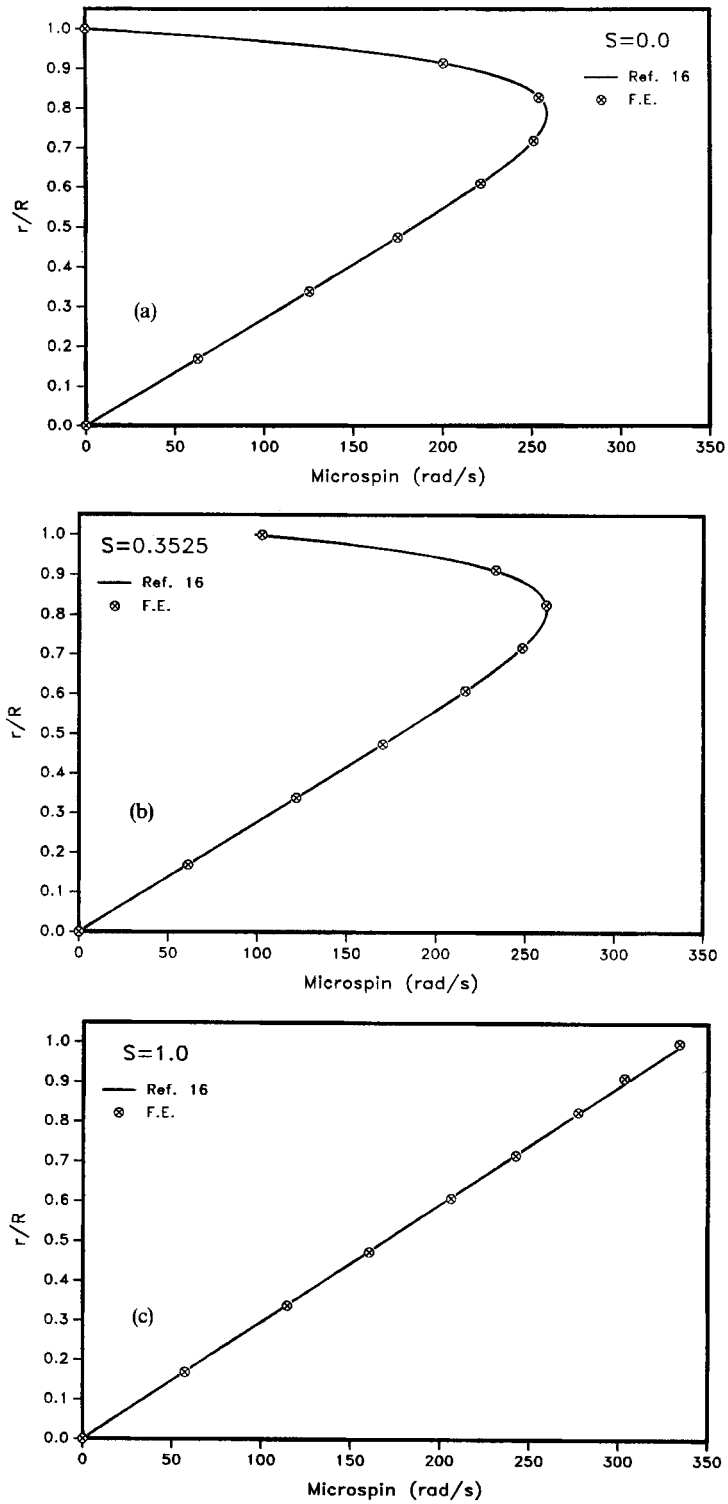

Figure 3. Microspin (v_θ) profiles for $S=0{\cdot}0$, $0{\cdot}3525$ and $1{\cdot}0$

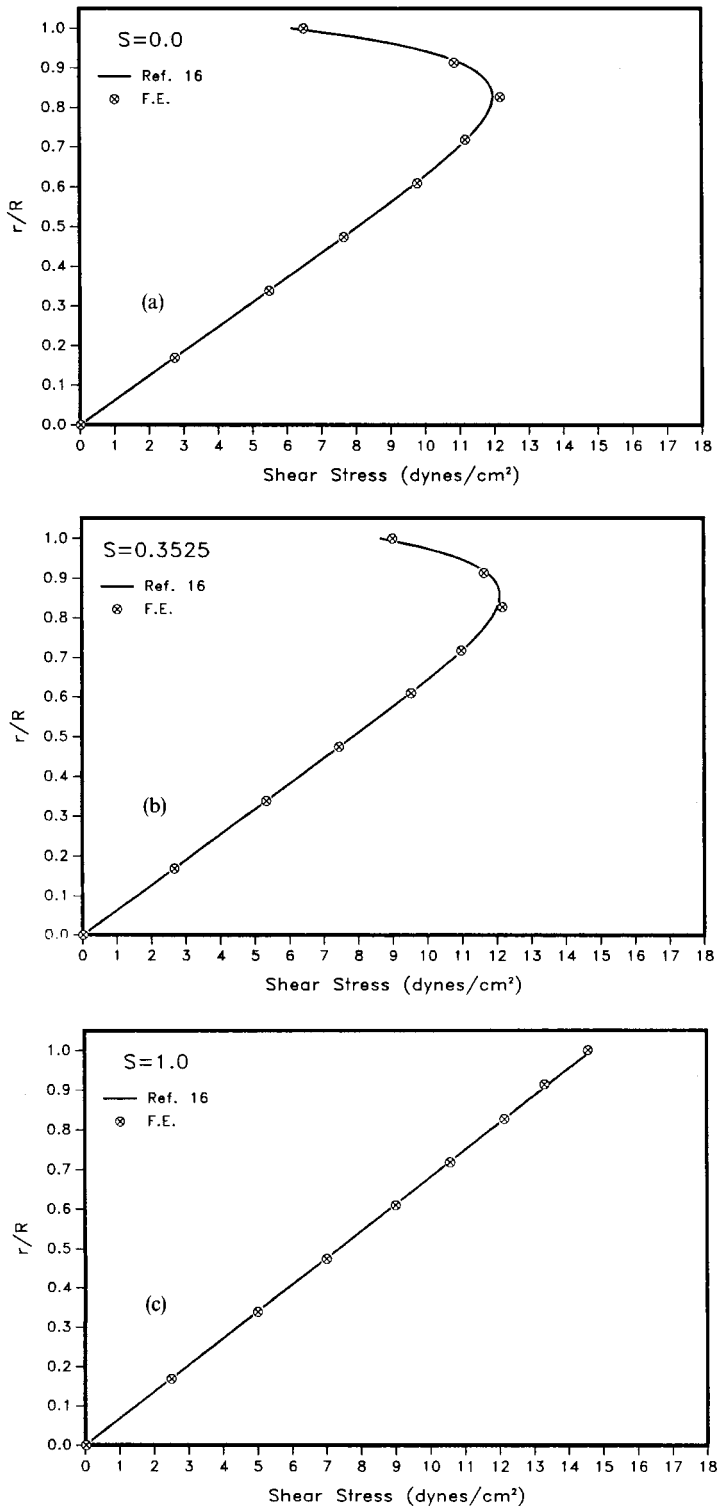

Figure 4. Shear stress (σ_{zr}) profiles for $S=0{\cdot}0$, $0{\cdot}3525$ and $1{\cdot}0$

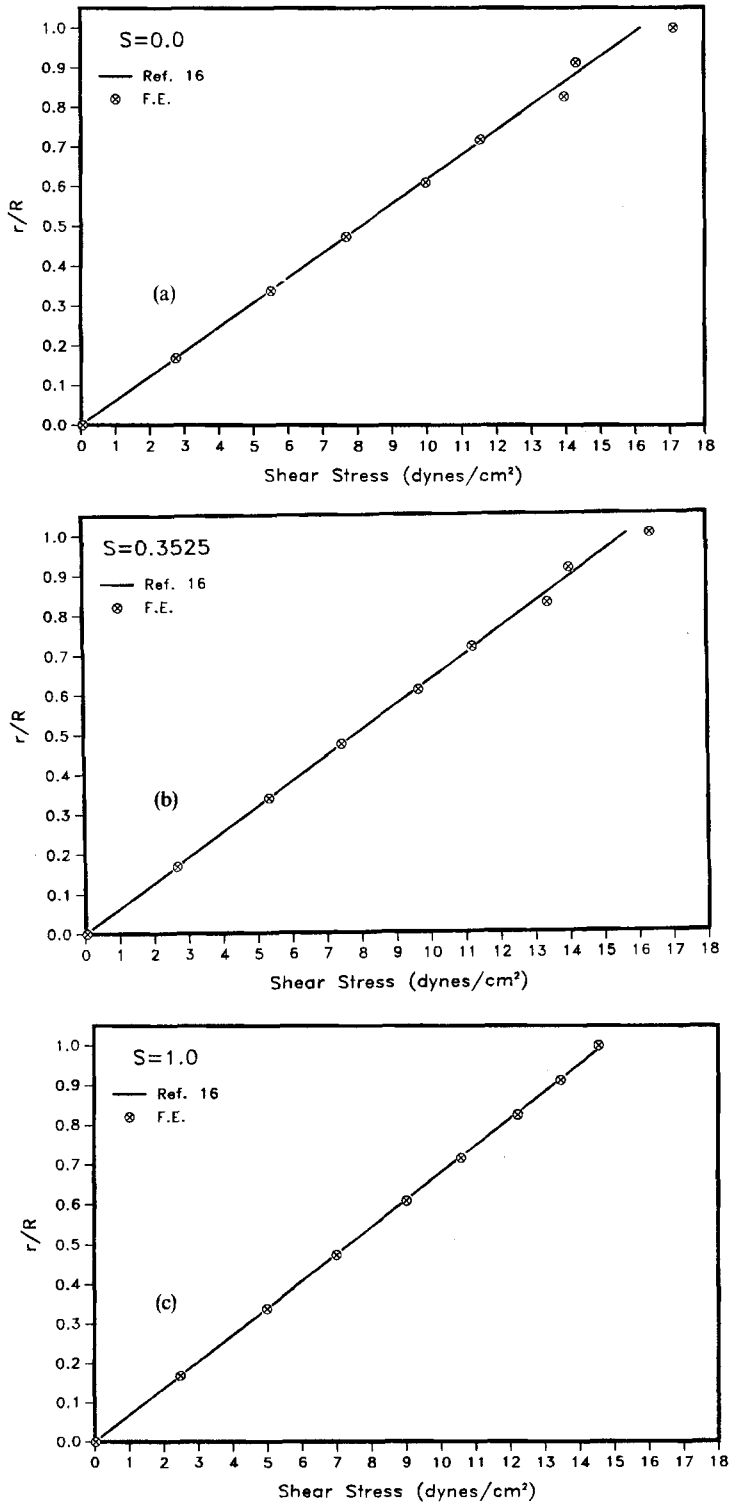

Figure 5. Shear stress (σ_{rz}) profiles for $S=0{\cdot}0$, $0{\cdot}3525$ and $1{\cdot}0$

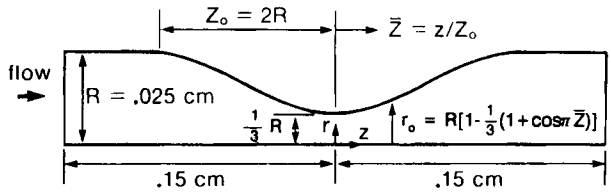

Figure 6. Constricted tube details

Table III. Summary of results for stenosis problem

Fluid type	Boundary condition parameter S	Inlet pressure (dyn cm^{-2})	Maximum wall shear stress (dyn cm^{-2})	Maximum axial velocity v_z (cm s^{-1})
Newtonian	—	3000	506·9	67·29
Micropolar	0·0	3627	644·2	71·23
Micropolar	0·1663	3540	622·7	70·75
Micropolar	0·3525	3435	596·9	70·13
Micropolar	0·8283	3150	525·6	68·53
Micropolar	1·0	3040	497·8	67·94

This problem has been examined in greater detail in studying the flow of blood through a stenosis or local narrowing of an artery.[34] Thus the constitutive constants are the same as given before in equation (55). The primary unknowns are again v_θ, v_r and v_z. Boundary conditions at the tube centreline and wall are the same as for the previous example, equations (54a)–(54c), with the exception that the solid boundary is now at $r=r_0$ rather than $r=R$, and r_0 is given by

$$r_0 = R \quad \text{for} \quad -3 \leqslant \bar{Z} \leqslant -1, \quad 1 \leqslant \bar{Z} \leqslant 3, \tag{57a}$$

$$r_0 = R\{1-\tfrac{1}{3}[1+\cos(\pi\bar{Z})]\} \quad \text{for} \quad -1 \leqslant \bar{Z} \leqslant 1. \tag{57b}$$

Inlet and outlet boundary conditions are likewise essentially the same as before, equations (54d) and (54e), but the inlet axial co-ordinate is now $z=-0{\cdot}15$ cm and the outlet $z=0{\cdot}15$ cm. The finite element mesh for the problem employs nine-noded Lagrangian elements with greater spatial refinement in the radial dimension near the vessel wall and in the axial dimension near the 'stenosis throat' (section of minimum radius at $\bar{Z}=0$).

Results and discussion. Results for several values of the microspin boundary condition parameter (S) are summarized in Table III and compared with results for a classical Newtonian fluid. The flow rate has again been maintained at $8{\cdot}27\times10^{-3}$ cm^3 s^{-1} for all cases. The driving pressures are included in Table III. The maximum wall shear stress is the largest value of the shear stress component acting on a plane tangent to the tube wall. This stress increases greatly as the tube diameter decreases and peaks slightly upstream from the stenosis throat. The maximum axial velocity occurs along the tube centreline ($r=0$) slightly downstream from the stenosis throat. Stresses and velocities for the micropolar fluid are generally higher than for the Newtonian fluid. The largest differences occur for $S=0$, in which case the maximum wall shear is 27% higher while the maximum velocity is only 6% higher.

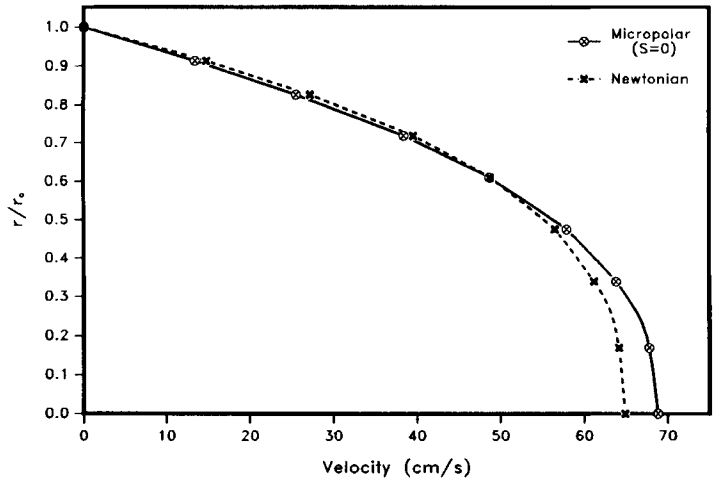

Figure 7. Axial velocity (v_z) profiles at stenosis throat ($\bar{Z}=0$)

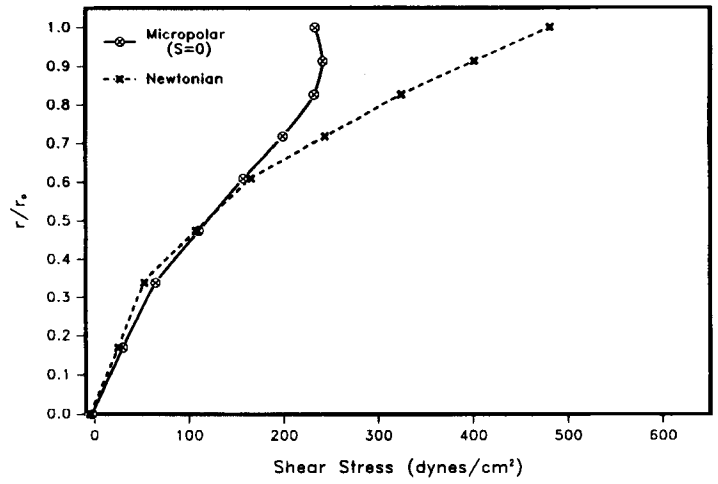

Figure 8. Shear stress (σ_{zr}) profiles at stenosis throat ($\bar{Z}=0$)

Further details of the solutions for the $S=0$ case are provided in the plots of Figures 7–9. Velocity profiles at the stenosis throat are compared in Figure 7. The greatest deviation between the micropolar and Newtonian solutions occurs at the tube centreline, where the axial velocity is about 6% higher for the micropolar fluid. The shear stress profiles in Figures 8 and 9 show more substantial differences (up to 50%) between micropolar and Newtonian solutions, particularly near the tube wall. These plots also highlight the asymmetry of the force stress tensor for micropolar fluids. An interesting finding from these results is that a micropolar fluid can exhibit a velocity profile quite similar to that of a Newtonian fluid yet have very different shear stresses. Stresses are more directly dependent upon velocity gradients and the relative rotation, or difference between fluid vorticity (ω_θ) and particle microspin (v_θ).

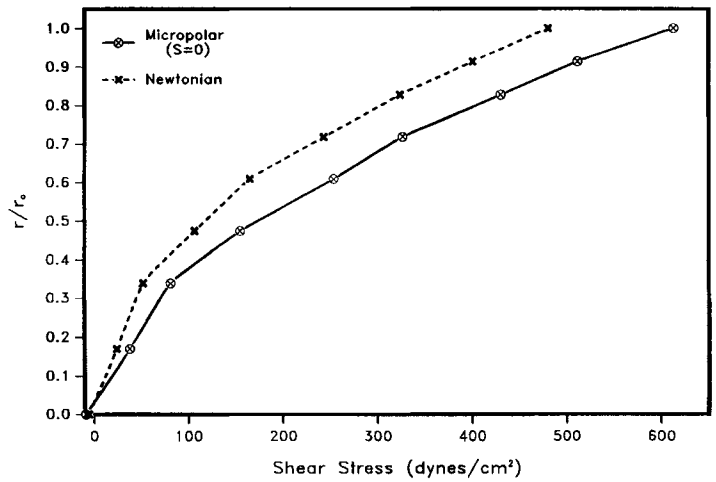

Figure 9. Shear stress (σ_{rz}) profiles at stenosis throat ($\bar{Z}=0$)

CONCLUDING REMARKS

The finite element formulation developed and demonstrated herein provides an effective numerical tool for solving problems involving the incompressible laminar flow of a class of fluids with microstructure. The specific case treated is that of micropolar fluids. The formulation includes an adjustable microspin boundary condition parameter for fluid microspin, which yields a flexible approach for examining a variety of solutions and assumptions. Solutions presented for the first sample problem agree quite well with analytical results. Greater accuracy could be obtained by refining the mesh accordingly. A major advantage offered by the finite element method is the ability to model flow through irregularly shaped regions. As an example, the formulation presented here has also been used to study blood flow through a stenosis or local vessel constriction, with blood modelled as a micropolar fluid. The method could be similarly applied to a variety of more general and complex problems involving the flow of fluids containing a solid particulate suspension phase.

REFERENCES

1. W. Voigt, 'Theoretical studies of the elastic behaviour of crystals', *Abhandlungen der Koniglichen Gesellschaft der Wissenschaften zu Gottingen*, **34**, (1887).
2. P. Duhem, 'Le potentiel thermodynamique et oa pression hydrostatique', *Ann. Ecole Normale*, **10**, 187–230 (1893).
3. E. Cosserat and F. Cosserat, *Theorie des Corps Deformables*. Hermann, Paris, 1909.
4. S. C. Cowin, 'Mechanics of Cosserat continua', *Ph.D. Dissertation*, Pennsylvania State University, 1962.
5. R. D. Mindlin and H. F. Tiersten, 'Effects of couple stresses in linear elasticity', *Arch. Rat. Mech. Anal.*, **11**, 414–448 (1962).
6. R. A. Toupin, 'Elastic materials with couple stress', *Arch. Rat. Mech. Anal.*, **11**, 385–414 (1962).
7. A. E. Green and R. S. Rivlin, 'Multipolar continuum mechanisms', *Arch. Rat. Mech. Anal.*, **17**, 113–147 (1964).
8. A. C. Eringen and E. S. Suhubi, 'Nonlinear theory of simple microelastic solids—I', *Int. J. Eng. Sci.*, **2**, 189–203 (1964).
9. A. C. Eringen, 'Theory of micropolar fluids', *J. Math. Mech.*, **15**, 1–18 (1966).
10. A. C. Eringen, 'Theory of micropolar elasticity', in H. Liebowitz (ed), *Fracture*, Academic, New York, 1968, pp. 621–729.
11. V. K. Stokes, 'Couple stresses in fluids', *Phys. Fluids*, **9**, 1709–1715 (1966).
12. M. E. Erdogan, 'Polar effects in apparent viscosity of a suspension', *Rheol. Acta*, **9**, 434–438 (1970).
13. T. Ariman, M. A. Turk and N. D. Sylvester, 'Microcontinuum fluid mechanics—a review', *Int. J. Eng. Sci.*, **11**, 905–930 (1973).

14. S. C. Cowin, 'The theory of polar fluids', in C. Yih (ed.), *Advances in Applied Mechanics Vol. 14*, Academic, New York, 1974, pp. 279–347.
15. V. K. Stokes, *Theories of Fluids with Microstructure*, Springer, Berlin, 1984.
16. P. Chaturani and S. P. Mahajan, 'Poiseuille flow of micropolar fluid with non-zero couple stress at boundary with applications to blood flow', *Biorheology*, **19**, 507–518 (1982).
17. P. Chaturani, V. S. Upadhya and S. P. Mahajan, 'A two-fluid model for blood flow through small diameter tubes with non-zero couple stress boundary condition at interface', *Biorheology*, **18**, 245–253 (1981).
18. K. C. Kang and A. C. Eringen, 'The effect of microstructure on the rheological properties of blood', *Bull. Math. Biol.*, **38**, 135–159 (1976).
19. A. S. Popel, S. A. Regirer and P. I. Usick, 'A continuum model of blood flow', *Biorheology*, **11**, 427–437 (1974).
20. T. Ariman, 'On the analysis of blood flow', *J. Biomech.*, **4**, 185–192 (1972).
21. K. C. Valanis and C. T. Sun, 'Poiseuille flow of a fluid with couple stress with applications to blood flow', *Biorheology*, **6**, 85–97 (1969).
22. K. A. Kline, S. J. Allen and C. N. DeSilva, 'A continuum approach to blood flow', *Biorheology*, **5**, 111–118 (1968).
23. V. K. Stokes, 'Couple stresses in fluids', *Phys. Fluids*, **9**, 1709–1715 (1966).
24. P. Sinha, C. Singh and K. R. Prasad, 'Lubrication of human joints—a microcontinuum approach', *Wear*, **80**, 159–181 (1982).
25. J. Prakash and P. Sinha, 'Lubrication theory of micropolar fluids and its application to a journal bearing', *Int. J. Eng. Sci.*, **13**, 217–232 (1975).
26. S. J. Allen and K. A. Kline, 'Lubrication theory of micropolar fluids', *J. Appl. Mech.*, **38**, 646–649 (1971).
27. J. Peddieson Jr., 'An application of the micropolar fluid model to the calculation of a turbulent shear flow', *Int. J. Eng. Sci.*, **10**, 23–32 (1972).
28. A. C. Eringen and T. S. Chang, 'A micropolar description of hydrodynamic turbulence', in A. C. Eringen (ed.), *Recent Advances in Engineering Science, Vol. 5/1*, Gordon and Breach, New York, 1968, pp. 1–8.
29. V. U. K. Sastry and V. R. M. Rao, 'Numerical solution of micropolar fluid flow in a channel with porous walls', *Int. J. Eng. Sci.*, **20**, 631–642 (1982).
30. G. Akay and A. Kaye, 'Numerical solution of time dependent stratified two-phase flow of micropolar fluids and its application to flow of blood through fine capillaries', *Int. J. Eng. Sci.*, **23**, 265–276 (1985).
31. J. N. Reddy, 'On the finite element model with penalty for incompressible fluid flow problems', in J. R. Whiteman (ed.), *The Mathematics of Finite Elements and Applications III*, Academic Press, London, 1979, pp. 227–235.
32. T. Ariman, M. A. Turk and N. D. Sylvester, 'On steady and pulsatile flow of blood', *J. Appl. Mech.*, **41**, 1–7 (1974).
33. G. Bugliarello and J. Sevilla, 'Velocity distribution and other characteristics of steady and pulsatile blood flow in fine glasss tubes', *Biorheology*, **7**, 85–107 (1970).
34. H. A. Hogan and M. Henriksen, 'An evaluation of a micropolar model for blood flow through an idealized stenosis', *J. Biomech.*, **22**, 211–218 (1989).